Environmental Science & Technology

Article

pubs.acs.org/est

Oxidative Remobilization of Technetium Sequestered by Sulfide-Transformed Nano Zerovalent Iron

Dimin Fan, Roberto P. Anitori,† Bradley M. Tebo, and Paul G. Tratnyek*

Institute of Environmental Health, Oregon Health & Science University, 3181 SW Sam Jackson Park Road, Portland, Oregon 97239, United States

Juan S. Lezama Pacheco

School of Earth Sciences, Environmental Earth System Science Department, Stanford University Stanford, Stanford, California 94305-4216, United States

Ravi K. Kukkadapu, Libor Kovarik, Mark H. Engelhard, and Mark E. Bowden

Environmental Molecular Sciences Laboratory, Richland, Washington 99354, United States

Supporting Information

ABSTRACT: Our previous study showed that formation of TcS_2-like phases is favored over TcO_2 under sulfidic conditions stimulated by nano zerovalent iron. This study further investigates the stability of Tc(IV) sulfide upon reoxidation by solution chemistry, solid phase characterization, and X-ray absorption spectroscopy. Tc dissolution data showed that Tc(VII) reduced by sulfide-transformed nZVI has substantially slower reoxidation kinetics than Tc(VII) reduced by nZVI only. The initial inhibition of Tc(IV) dissolution at S/Fe = 0.112 is due to the redox buffer capacity of FeS, which is evidenced by the parallel trends in oxidation−reduction potentials (ORP) and Tc dissolution kinetics. The role of FeS in inhibiting Tc oxidation is further supported by the Mössbauer spectroscopy and micro X-ray diffraction data at S/Fe = 0.112, showing persistence of FeS after 24-h oxidation but complete oxidation after 120-h oxidation. X-ray absorption spectroscopy data for S/Fe = 0.011 showed significantly increasing percentages of TcS_2 in the solid phase after 24-h oxidation, indicating stronger resistance of TcS_2 to oxidation. At S/Fe = 0.112, the XAS results revealed significant transformation of Tc speciation from TcS_2 to TcO_2 after 120-h oxidation. Given that no apparent Tc dissolution occurred during this period, the speciation transformation might play a secondary role in hindering Tc oxidation. Collectively, the results indicate that sequestrating Tc as TcS_2 under stimulated sulfate reduction is a promising strategy to improve the long-term stability of reduced Tc in subsurface remediation.

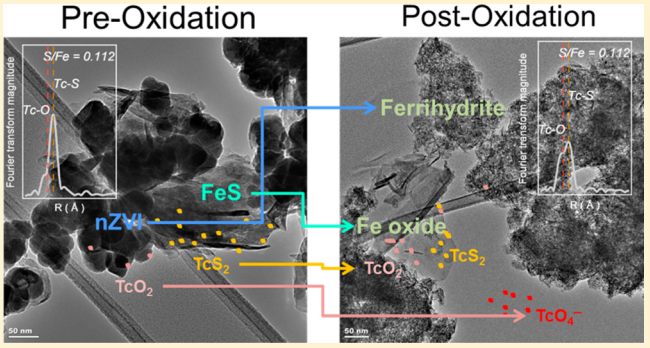

INTRODUCTION

Technetium-99 (^{99}Tc) is a common radioactive contaminant of groundwater at nuclear waste reprocessing sites.[1,2] The environmental risk of Tc arises primarily from its long half-life and high mobility as pertechnetate oxyanion ($Tc^{VII}O_4^-$) under oxic groundwater conditions.[3] Under anoxic conditions, the solubility and mobility of Tc are much less because $Tc^{VII}O_4^-$ is readily reduced to the relatively insoluble oxide, $Tc^{IV}O_2{\cdot}nH_2O$ (log K_{sp} = −8.4[4]) by a variety of abiotic and biotic processes. Many studies have suggested that dissimilatory iron reduction is the predominant biogeochemical process mediating the reductive sequestration of Tc[5−8] and that enhanced rates of Tc sequestration can be achieved with abiotic reductants like adsorbed Fe(II)[9−13] or Fe^0.[14] The resulting $Tc^{IV}O_2{\cdot}nH_2O$ can be sequestered by adsorption onto mineral surfaces,[10] incorporation into mineral lattice structures,[15] or association with organic matter.[16]

The long-term benefit of Tc sequestration by reduction, however, remains uncertain due to the high susceptibility of $Tc^{IV}O_2{\cdot}nH_2O$ to reoxidation. The reoxidation of reduced Tc oxide occurs when oxic groundwater or seawater intrudes into anoxic aquifers contaminated with Tc,[17] or when Tc-bound sediments are resuspended above the oxic-anoxic interface during seasonal redox cycling of the subsurface.[18] Although oxygen is generally considered to be the major cause of Tc

Received: April 1, 2014
Revised: May 31, 2014
Accepted: June 2, 2014
Published: June 2, 2014

reoxidation, other naturally occurring oxidants can also oxidize Tc(IV). Such oxidants include nitrate,[18,19] which is a common cocontaminant with Tc, and Mn(IV) oxides, which is an oxidant mainly of biogenic origin that recently has received substantial interests for its role in oxidizing UO_2.[20−24] The former process is coupled with microbial nitrate reduction with Tc(IV) oxide as the electron donor, while the latter reaction is mediated via solid-phase electron transfer.[22,23] Nevertheless, the rate of Tc reoxidation driven by these processes—at least as observed at the laboratory scale—is much slower than O_2-promoted oxidation.[19]

Enhanced stability of reduced Tc oxides against reoxidation has been observed when they are closely associated with host minerals.[10,15,25] This benefit was attributed to (i) formation of a protective layer that physically blocks oxygen diffusion to $Tc^{IV}O_2{\cdot}nH_2O$ and (ii) additional redox buffer capacity provided by host minerals (e.g., scavenging potential oxidants of Tc by structural Fe(II)), and (iii) incorporation of Tc(IV) into the lattice structures of the host minerals. However, the extent of stabilization varies substantially among different studies and appears to depend on the physical and chemical properties of host minerals and the specific experimental conditions under which reduced Tc is formed. For example, Frederickson et al.[25] compared the reoxidation rates of Tc reduced by two different iron-reducing sediments, and found a significantly slower Tc reoxidation rate for one material. They postulated that the slower and incomplete Tc oxidation was due to limited oxygen diffusion to Tc protected within aggregates that were only present in the less reactive sediment. In another study, Um et al.[15] reported that Tc(IV) reduced by Fe(II)-sorbed goethite exhibited strong resistance to reoxidation. However, in their experiments, the Tc-goethite mixture was annealed at 80 °C for 7 days to promote Tc substitution and incorporation into goethite structure. In general, Tc reduced by anaerobic sediments in microcosm studies seems to be more susceptible to oxidation than Tc reduced by pure or synthetic minerals. It is likely that the heterogeneity of natural sediments may favor the prevalence of labile Tc-mineral associations (e.g., physical adsorption) as opposed to relatively more stable associations with pure mineral phases (e.g., chemical adsorption or incorporation).

Given the high susceptibility of Tc oxides to oxidation, we have investigated an alternative strategy to sequester Tc as Tc sulfide by stimulating sulfidic conditions with nano zerovalent iron (nZVI). We recently showed that the sequestered Tc formed in this way is mainly composed of TcS_2-like phase.[26] Another recent study also reported the presence of TcS_2-like phases in microbially reduced hyporheic zone sediment, demonstrating the presence of Tc sulfide under less extreme environmental conditions.[27] On the basis of previous studies conducted under various conditions (mostly high pH and ionic strength to simulate waste leachate), reduced Tc sulfide phases, including TcS_2 and Tc_2S_7, appeared to be more resistant against oxidation.[28−31] The reoxidation rates of Tc_2S_7 by O_2 reported by Lukens et al.[30] and Liu et al.[28] are substantially slower than that of $TcO_2{\cdot}nH_2O$ reported elsewhere.[18,25] It was also shown that the TcS_2-like phases formed by coprecipitation with FeS transformed to $TcO_2{\cdot}nH_2O$ without being further oxidized to Tc(VII) in damp air.[31] Given the similar size of Tc(IV) and Fe(III) and the octahedral binding structure of both atoms to oxygen, the authors suggested that possible incorporation of Tc(IV) into the lattice structure of goethite—the oxidation product of FeS—stabilizes Tc(IV).

As a follow up to our previous work showing facile reductive sequestration of Tc by nZVI under sulfidic conditions, this study was performed to investigate the stability of the sequestration products with respect to oxidative dissolution. The primary goal was to characterize the changes in speciation of Tc during the reoxidation process under environmentally relevant conditions. However, because our prior work had demonstrated that secondary FeS (formed during sulfidation) is an important sink for Tc sequestration, this study also addressed changes in the host mineral composition (e.g., FeS) during oxygenation of the sample and its effects on Tc remobilization. The results confirm that reduced S containing phases of Tc and Fe contribute to the stability of Tc sequestration products, and therefore that this might form the basis for an improved strategy for remediation of technetium contaminated groundwater.

EXPERIMENTAL SECTION

Chemical Reagents. All reagents were reagent grade and used as received without further purification. ^{99}Tc was obtained as concentrated stock solution of ammonium pertechnetate (NH_4TcO_4) from Pacific Northwest National Laboratory. ^{99}Tc is a radioactive β emitter (half-life = 2.13×10^5 years; E_{max} = 294 keV) and was handled in a properly equipped radioactive laboratory.

Tc Reoxidation Experiments. Tc reoxidation was conducted following the conclusion of Tc reduction experiments. The latter were carried out as described previously.[26] Briefly, freshly prepared nZVI (0.2−0.5 g L^{-1}) was pre-equilibrated with various concentrations of sulfide (S/Fe molar ratio = 0−1.12) in 10 mL deoxygenated artificial Hanford groundwater HS300[32] (pH buffered at 7.8 with 30 mM HEPES, Chemical compositions shown in Table S1 in the Supporting Information (SI)) under anaerobic conditions for 24 h. TcO_4^- was then added to a final concentration of 6 μM. After >99% removal of aqueous Tc (<0.2 μm fraction), the reactors were left aging for different periods of time (7 days or 9 months) before reoxidation was initiated.

The reoxidation experiments were carried out by bubbling 0.2 μm filtered air into a water trap bottle, which then passed to the suspension via a 21 gauge needle through a butyl rubber septum (Bellco Glass; Vineland, NJ). The air bubbling rate (~2−3 bubbles/sec) was adjusted to provide gentle mixing of the solid and aqueous phases. No additional mixing was applied. For sampling, 0.3 mL of suspension was withdrawn from the reactor and passed through a 0.2 μm filter preflushed with N_2, and the Tc concentration in the filtrate was measured by liquid scintillation counter (Beckman; Brea, CA). Water loss due to evaporation was monitored by weighing reactors between each sampling and was found to be negligible.

Reoxidation of Host Minerals. To understand the evolution of host mineral phases during reoxidation, parallel Tc-free reoxidation experiments were conducted after 0.5 g L^{-1} nZVI was equilibrated with 0 and 1 mM sulfide for 7 days (S/Fe = 0 and 0.112). The procedure was the same as for the Tc reoxidation experiments, except that a large volume 50 mL reactor was used in order to provide a sufficient quantity of solids for material characterizations. During oxidation, the oxidation−reduction potential (ORP) of the suspension was measured intermittently with a Pt microelectrode with Ag/AgCl as a reference electrode. After 0, 24, 120, and 312 h of oxidation, the reactors were sacrificed, and the solids were recovered by vacuum filtration inside an anaerobic chamber

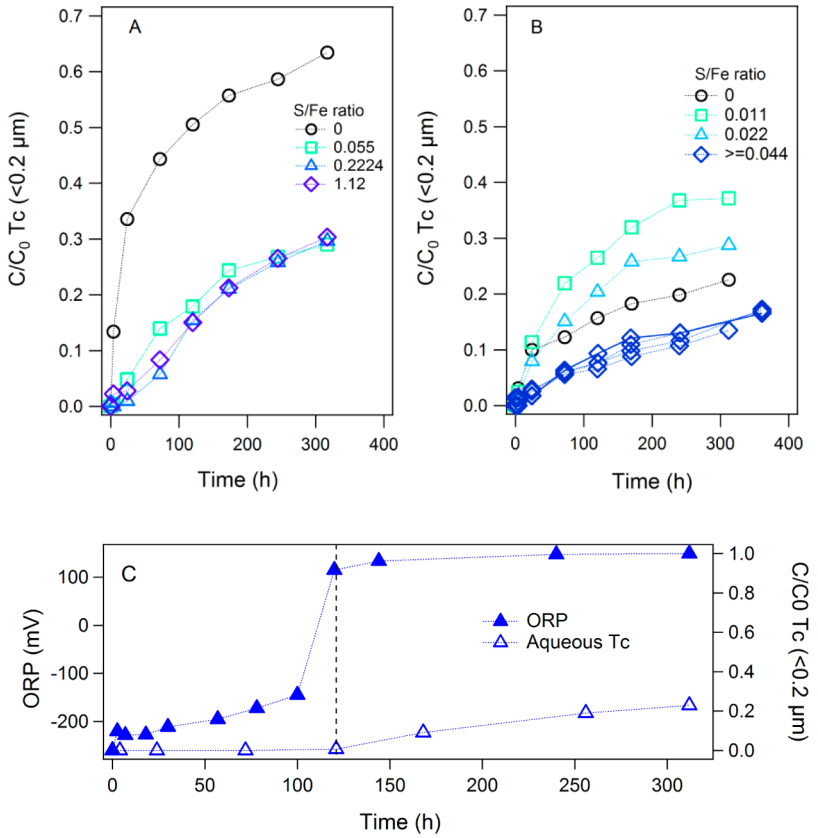

Figure 1. (A) Aqueous Tc reappearance kinetics of 7-day aged samples in 10 mL batches; (B) Tc reoxidation kinetics of 9-month aged samples in 10 mL batches; and (C) ORP and aqueous Tc concentration vs time during reoxidation in the 50 mL batch reactor at S/Fe = 0.112 aged for 7 days.

following the procedure described elsewhere.[33] The solids were then sealed under N_2 atmosphere and delivered to the Environmental Molecular Sciences Laboratory (EMSL, Richland, WA) for characterization.

Solid Phase Characterization. Preliminary characterization by Mössbauer spectroscopy on oxidized samples, with or without exposure to Tc, showed that Tc at the concentration used in this study has no detectable effect on the oxidation products of the host minerals. Therefore, further solid phase analysis was done with Tc-free samples for convenience. The bulk mineralogy of sulfidated nZVI throughout the oxidation process was characterized by micro X-ray diffraction (μXRD) and Mössbauer spectroscopy. The near-surface composition of the material was analyzed by X-ray photoelectron spectroscopy (XPS). The microscopic structures of the mineral phase were examined by transmission electron microscopy (TEM) with energy dispersive X-ray spectroscopy (EDS). Details for these methods are given in the SI.

X-ray Absorption Spectroscopy. Samples were prepared with the solids containing Tc freshly reduced by 0.5 g L^{-1} nZVI that was pretreated with 0, 0.1, and 1 mM sulfide (S/Fe: 0, 0.011, and 0.112) in 50 mL batch reactors. The reduced solids were further oxidized for 0, 24, 120, and 312 h, 7 days after Tc reduction completed. After oxidation, the solids were recovered by centrifugation and then loaded as a concentrated slurry/paste into single slot Teflon holders. The holders were then sealed with a single layer of Kapton tape and further contained inside a heat-sealed polypropylene bag. Additional samples that were aged in solution were also prepared for XAS following the same procedure. Details of those samples are given in SI. Loaded samples were kept in an anaerobic chamber prior to the measurements.

Tc K-edge XAS data were collected at the Stanford Synchrotron Radiation Lightsource (SSRL) on beamline 4−1 and 11−2. Spectra were measured at room temperature under a continuous He purge in fluorescence mode using a 13 (30) element solid state detector (Ge), and a N_2-cooled Si (220) double crystal monochromator, detuned 20% for harmonic rejection. Energy calibration was internally measured during each scan using a Mo metal foil (Mo K-edge energy 20000.0 eV). EXAFS spectra were analyzed using SixPack, Athena, and Artemis interfaces to the IFEFFIT package. Backscattering phase and amplitude functions required for fitting individual scattering contributions of spectra were obtained from FEFF8.

RESULTS AND DISCUSSION

Tc Reoxidation Kinetics. The reoxidation kinetics of freshly reduced Tc in 10 mL batch reactors is shown in Figure 1A. In the absence of sulfide, aqueous Tc rapidly increased during the initial 20-h oxygenation, presumably due to oxidative dissolution. After 20-h oxidation, the aqueous Tc appearance rate slowed, and appeared to gradually approach a plateau by 312-h oxidation. By the end of the experiments, approximately 30% of the Tc still remained associated with the solid phases, possibly because residual Tc phases that were more resistant to oxidation formed as oxidation progressed. This could be due to either Tc incorporation into the lattice structures of oxidized Fe mineral phases[15,31] or formation of secondary iron minerals that protect reduced Tc from oxidation. In the presence of sulfide, the Tc reappearance rate was significantly slower compared to the absence of sulfide. However, among three

dx.doi.org/10.1021/es501607s | Environ. Sci. Technol. 2014, 48, 7409−7417

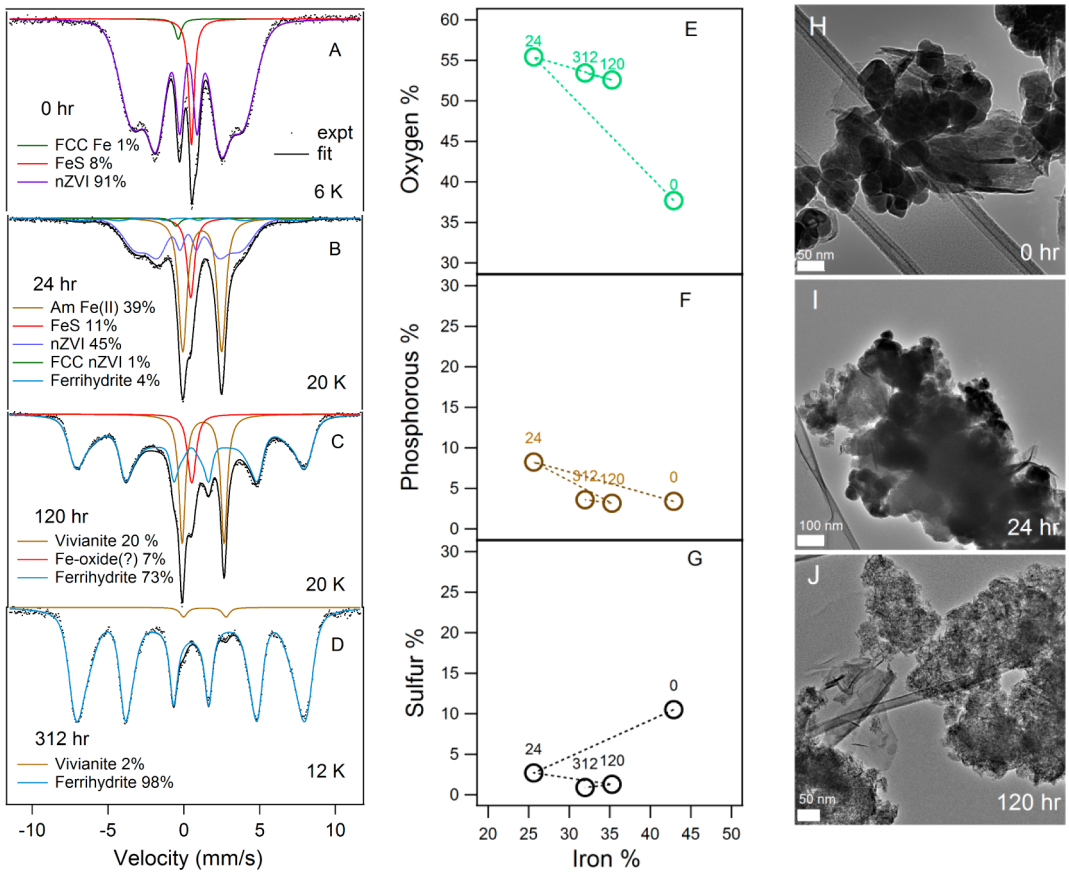

Figure 2. Solid phase characterizations of sulfidated nZVI (S/Fe = 0.112) during oxidation. Left panel: Experimental and modeled Mössbauer spectra of sulfidated nZVI after (A) 0, (B) 24, (C) 120, and (D) 312-h oxidation (FCC: face cubic center); Middle panel: XPS wide survey plot of surface atomic percentage of (E) oxygen, (F) phosphorus, (G) sulfur vs Fe during oxidation (numbers in E, F and G represent oxidation time; Sulfur refers exclusively to S^{2-}); Right panel: transmission electron micrographs of sulfidated nZVI after (H) 0, (I) 24, and (J) 120-h oxidation (associated EDS spectra are presented together with TEMs in SI Figure S5). All data for the 0-h oxidized sample are adopted from Fan et al.[26]

different S/Fe ratios (0.055, 0.224, and 1.12) that were tested initially, no appreciable difference of aqueous Tc concentration after 312-h oxidation was observed.

The trend in reoxidation kinetics observed in the presence and absence of sulfide is consistent with the speciation of reduced Tc produced across a range of S/Fe ratios that was reported in our reduction study.[26] In that work, we showed that TcO_4^- was directly reduced by nZVI to $TcO_2{\cdot}nH_2O$ in the absence of sulfide. With increasing sulfide doses—even at relatively low S/Fe ratios—a TcS_2-like phase quickly became the dominant reduced Tc species due to the high affinity of FeS for TcO_4^-. The slower kinetics of Tc reoxidation in the presence of sulfide appears to confirm the hypothesis that TcS_2-like phases are more resistant to oxidation than TcO_2. The lack of difference in Tc reoxidation kinetics at three S/Fe ratios also agrees with the finding that TcS_2 is the major component of reduced Tc species above S/Fe = 0.05.[26]

To test the effects of aging, reoxidation was also conducted on reduced Tc that was aged for 9 months (Figure 1B). Similar to freshly reduced samples, no appreciable difference in reoxidation kinetics was observed at S/Fe ratios above 0.044. However, at the two lowest S/Fe ratios tested (0.011 and 0.022)—where the percentage of TcO_2 formed was significantly higher[26]—Tc reoxidation was correspondingly faster and the kinetics seems to be positively correlated with the S/Fe ratio. This further indicates that TcS_2 is less labile to oxidation compared to TcO_2. It is noteworthy that the nZVI only sample aged for 9 month had slower reoxidation kinetics than S/Fe = 0.011 and 0.022. This result was not replicated and the reasons for it were not investigated, but it could arise from geochemical stabilization developed during the aging process. In fact, all of the 9-month aged samples at S/Fe > 0.044 had considerably slower reoxidation kinetics (Figure 1B) than their freshly reduced counterparts (Figure 1A).

Close inspection of the reoxidation kinetics of fresh samples (Figure 1A) shows that at relatively high S/Fe ratios (S/Fe = 0.22 and 1.12), there was an initial lag period of about 24 h during which little aqueous Tc was detected. By contrast, a relatively large fraction of reduced Tc was remobilized within 2 h after O_2 introduction in the absence of sulfide. A lag phase was also observed for uraninite oxidation in the presence of FeS,[34] and was attributed mainly to FeS being a redox buffer that scavenged dissolved O_2 (although the possibility of oxidized U being rereduced by Fe(II) was not excluded). Given that our previous study demonstrated that FeS is formed and this phase is responsible for sequestration of Tc as TcS_2,[26] the observed lag in initial Tc oxidation is most likely caused by FeS. It is also worth noting that the two highest S/Fe ratios did not result in longer lag phases, which is consistent with our prior finding[26] that FeS formation was inhibited at higher S/Fe ratios, presumably due to limited nZVI surface sites.

Parallel measurements of ORP and Tc dissolution in the 50 mL batch reactor (for the purpose of preparing XAS samples) at S/Fe = 0.112 further confirms the role of FeS in inhibiting

dx.doi.org/10.1021/es501607s | Environ. Sci. Technol. 2014, 48, 7409−7417

initial Tc oxidation by showing that (i) the lag period where Tc dissolution was inhibited was extended to ~120 h (compared to ~20 h in 10 mL batches), presumably because of the higher quantity of FeS in the larger reactor (Figure 1C); and (ii) the onset of active Tc dissolution occurred after a sharp rise in ORP from −150 to 100 mV around 120 h (Figure 1C). Although interpreting ORP data in our system is complicated by the presence of both dissolved and solid phase redox-active species,[35] the steep ORP rise at 120 h most likely reflects the depletion of reducing capacity contributed by nZVI and FeS due to reaction with dissolved oxygen. In fact, analogous ORP profiles have been observed in other studies where FeS was oxidized by oxygen,[34,36] and a similar concurrency between sharply increased ORP and uranium remobilization has been observed.[34]

Oxidation of Host Mineral Phases. Further investigation into the mineralogical transformations of the host minerals during oxidation was conducted at S/Fe = 0 and 0.112. Because the main focus of this study was on sulfidated nZVI, all characterizations of unsulfidated nZVI (S/Fe = 0) for comparison are presented in the SI (Figure S1−S2). The S/Fe ratio of 0.112 was chosen because our reduction study showed that this is the optimal S/Fe ratio in batch experiments to maximize FeS formation (higher S/Fe ratio did not result in more FeS formation) and to sequester Tc primarily as TcS_2.[26]

The μXRD of all oxidized samples was dominated by broad and indistinct features (SI Figure S1), in agreement with amorphous nature of the fully reduced starting material.[26] Minor peaks due to the following phases were also evident (SI Figure S1B): (i) mackinawite in 0, and 24 h samples, (ii) vivianite in 120 h sample (due to 1.5 mM phosphate in HS300), and (iii) broad peaks due to ferrihydrite-like mineral in 24, 120, and 312 h samples (ferrihydrite-like mineral content increased with oxidation time). Mössbauer spectroscopy measurements were used to quantify *bulk* changes in both nZVI and FeS components, together with evolved oxidized Fe mineral phases, during oxidation (Figure 2A−D). Prior to oxidation, the bulk solid was composed of ~8% mackinawite—the low spin (LS) Fe(II)-tetrahedral-compound shown as red singlet—and 92% nZVI, based on the Mössbauer characterization in our previous study (also shown in Figure 2A).[26]

After 24-h oxidation, the FeS singlet retained in the 20-K Mössbauer spectrum (Figure 2B), and the presence of FeS was further confirmed by multiple peaks that match mackinawite in μXRD (SI Figure S1B) and by TEM-EDS, showing the presence of typical FeS morphology with a S/Fe ratio close to 1 (SI Figure S5A). Nevertheless, XPS survey scan data on the 24-h oxidized sample indicated significant decrease of S^{2-} intensity (Figure 2E) and the Fe 2p narrow spectra (SI Figure S4A) also showed strong attenuation of the Fe(II)-S peak around 706.6 eV, both of which suggest the disappearance of reduced sulfide near the mineral surface. These results are consistent with prior studies showing significant FeS dissolution at the beginning of oxidation around acidic to neutral pH values.[37] A qualitative Mössbauer modeled fit (SI Figure S3) further revealed possible Fe(III) structures that might result from structural and surface oxidation of FeS.[34]

The main oxidized Fe species emerged after 24-h oxidation was high spin (HS) Fe(II), represented by a broad Fe(II) doublet in the 20-K Mössbauer spectrum (Figure 2B). The formation of Fe(II) primarily resulted from oxidation of nZVI as the reduction in the percentage of nZVI (from 92% to 45%) corresponded well with the formation of HS Fe(II) (39%), although a small fraction of Fe(II) could also have resulted from FeS oxidation. The nature of this HS Fe(II) phase, however, remains unclear. The XPS survey scan of the 24-h oxidation sample showed a large increase of P and O near the surface with decreased Fe (Figure 2E and F). Additionally, TEM (Figure 2I) showed that the exterior of mineral aggregates was mostly composed of less electron dense materials, which are enriched in P and Ca relative to the interior regions that are Fe rich (see EDS spectra, SI Figure S5A). However, no vivianite ($Fe_3(PO_4)_2{\cdot}8H_2O$) peaks were identified by μXRD (SI Figure S1). It is possible that at the early stage of oxidation, secondary mineral phases formed by dissolution, oxidation, and reprecipitation still mostly preserve the amorphous or nanocrystalline nature of the starting material. A small percentage of ferryhydrite (4%) was also identified by the modeled Mössbauer spectrum (the broad sextet in Figure 2B), presumably due to oxidation.

Further oxidation to 120 h resulted in more complete oxidation of host minerals. The fitting of the Mössbauer 20-K spectrum indicated that the percentage of ferrihydrite increased to 73% while the HS Fe(II) percentage decreased to 20% (Figure 2C). The residual high spin Fe(II) underwent further crystallization to form vivianite, which is supported by Mössbauer fitting parameters (SI Table S2) and μXRD (SI Figure S1B). A third component resembled the singlet feature of low spin Fe(II)S, but FeS peaks were not evident in the μXRD pattern (SI Figure S1B). Further examination of the Mössbauer fitting parameters showed slight deviations from the FeS component in the 0 and 24-h oxidized samples (SI Table S2). TEM (Figure 2J) showed that apart from the major structure that is composed of poorly crystalline small particles (presumably ferrihydrite based on the μXRD data), a small fraction of the solid materials exhibit the distinctive ribbon-like structure that is typical of mackinawite (Figure 2J and SI Figure S5C). The EDS, however, showed only Fe and O as the main elements with no or very low levels of sulfur (SI Figure S5B). It is possible that these structures were some transient phases of FeS oxidation (which likely caused the unidentified Mössbauer component with similar singlet shape to FeS in the 120-h oxidation sample) and had yet to be transformed to more stable phases. This might also indicate that the Fe atoms in nZVI and FeS were oxidized to different phases. By 312-h oxidation, the solid phase was nearly completely transformed to ferrihydrite, based on Mössbauer (Figure 2D) and μXRD data (SI Figure S1B).

Despite FeS only being a minor component of sulfidated nZVI (8% of the total solid based on Mössbauer fitting of the 0-h oxidation sample), its oxidation plays an important role in Tc remobilization because it is the major mineral phase that associated with Tc sulfide.[26] The effect of the oxidation of iron sulfide minerals on contaminant remobilization, including heavy metals and oxyanions, has been the subject of many studies.[34,37−41] Among various biotic and abiotic oxidizing agents, oxygen is of particular interest due to its ubiquitous role in chemical oxidation. The general consensus on the mechanism of abiotic oxidation of FeS by oxygen is that iron and sulfur undergo independent oxidations to form Fe (oxyhydr)oxide and elemental sulfur (polysulfide) as the main products, respectively. At neutral pHs, the oxidation of FeS was suggested to proceed via solution phase oxidation and solid phase mediated oxidation mechanisms.[34,37] Given that our study was conducted under comparable conditions (e.g., near neutral pH), it is expected that the oxidation of FeS component

in the current study follows the same pathway, despite the lack of complementary solution chemistry data. The absence of a strong polysulfide/elemental sulfur signal in our S2p XPS narrow scan (SI Figure S4B) could be because these spectra were collected at room temperature, which can cause sublimation of S^0 under high vacuum.[42] The difference in the iron mineralogy of the final oxidation product between this study and prior work might be largely due to variations in geochemical conditions (e.g., aqueous constituents).

Evolution of Tc Speciation. Both Tc reappearance kinetics and mineral characterizations suggest that the redox buffer capacity of sulfidated nZVI plays a key role in inhibiting initial Tc reoxidation. However, slower Tc reoxidation was also observed at the final stage of the batch experiments with sulfidated nZVI, even when the redox buffer capacity should have been depleted by extended exposure to oxygen (Figure 1A). Recalling that the reduction study showed that Tc was sequestered mainly as TcS_2 in the presence of sulfide,[26] it is possible that Tc speciation might be another reason for slower Tc reoxidation in the presence of sulfidated nZVI.

To further investigate the factor(s) that regulates Tc remobilization, X-ray absorption spectroscopy (XAS) measurements were performed to probe the change in speciation of reduced Tc during reoxidation. Tc K-edge data were collected on the solids of S/Fe = 0, 0.011, and 0.112 recovered after 0, 24, 120, and 312-h oxidation. In the absence of sulfide, both XANES (SI Figure S6A) and EXAFS (SI Figure S6B) showed that solid Tc speciation (S/Fe = 0) remained nearly unchanged throughout the oxidation process. Because the aqueous phase was mostly removed during XAS sample preparation, no oxidized Tc ($Tc(VII)O_4^-$) was observed (in contrast to the results described in Lukens et al.[30]). The Tc speciation was consistent with $TcO_2{\cdot}2H_2O$ shown in the reduction study,[26] along with many prior studies.[10,14,43]

The Tc reduction study showed that the speciation of reduced Tc at different S/Fe ratios can be represented by a mixture of TcO_2 and TcS_2, and that the Tc absorption edge position can be used as an indicator to qualitatively assess the respective content of TcS_2 and TcO_2 in a given mixture (because the former has about 6 eV lower absorption edge than the latter, even though both are Tc(IV) species).[26] In this study, at S/Fe = 0.011, the Tc absorption edge decreased from ca. 21059.2 to ca. 21056.6 eV after 24-h oxidation (Figure 3). This shift in the absorption edge position suggests an increasing percentage of TcS_2 after 24-h oxidation. This was further confirmed by increasing intensity for Tc—S binding in the Fourier transformed EXAFS (Figure 4B) and higher TcS_2 content based on linear combination fitting (Figure 4C). Given that little inhibition of Tc dissolution was observed at low S/Fe ratios—presumably due to minimal FeS formation—the increase in the TcS_2 percentage likely suggests that more TcO_2 relative to TcS_2 was oxidized to aqueous Tc(VII). After 120-h oxidation, the absorption edge, however, increased back to the level similar to that seen in the 0-h oxidation sample and the Tc—S peak attenuated in the Fourier transformed EXAFS spectrum (Figure 4B), indicating that TcS_2 was gradually oxidized (or transformed), leaving higher TcO_2 percentage in the solid phase.

At S/Fe = 0.112, the fully reduced Tc was mainly present as TcS_2 (>90% based on LCF of EXAFS data in Figure 4C). The initial 24-h oxidation resulted in little change of the overall Tc speciation as the absorption edge position remained at 21053 eV (Figure 3) and the EXAFS of the 0-h and 24-h oxidation

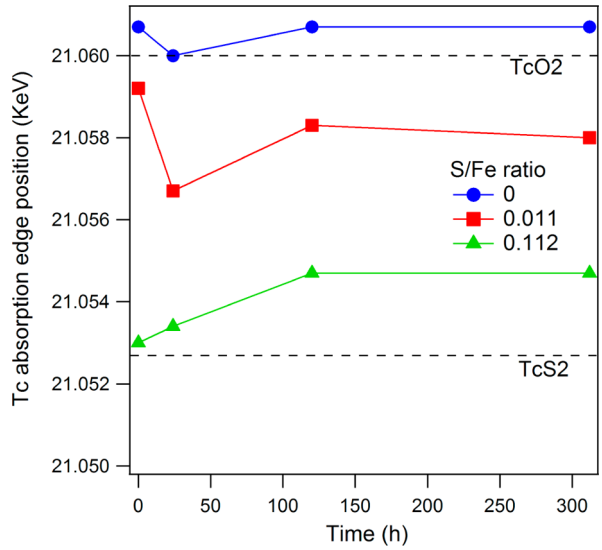

Figure 3. Tc XANES absorption edge positions during oxidation at S/Fe = 0, 0.011, and 0.112 (The values for the 0-h oxidized samples, TcO_2, and TcS_2 (dashed lines) are adopted from our Tc reduction study[26]).

samples were almost identical (Figure 4A). Because no significant Tc dissolution occurred during the initial 24 h (Figure 1C), little or no speciation change indicates that the presence of redox buffer capacity protected reduced Tc from oxidation. This is consistent with the solid phase characterization, showing substantial surface oxidation of the host minerals during the initial 24 h (Figure 2E–G). After 120-h oxidation, a significant change of solid Tc speciation was evident by XAS: (i) the absorption edge position increased by ~2 eV (Figure 3) and (ii) the Fourier transformed EXAFS showed notable enhancement of the Tc—O peak at the expense of a decreasing Tc—S peak (Figure 4B). Recall that the kinetic data still did not show elevated aqueous Tc concentration by this time point. Therefore, the substantially increasing percentage of TcO_2 in the solid phase could only have resulted from a change of Tc speciation in TcS_2 to TcO_2. A similar transformation from Tc sulfide to Tc oxide was reported for the oxidation of TcS_2-like phases in damp air in the presence of FeS.[31] However, in contrast with that study, where Tc(IV) was shown to be eventually incorporated into goethite structure, we found little evidence of Tc incorporation into the iron oxide or ferrihydrite mineral in this study (including Fe(II) in the second shell did not significantly improved the overall fitting). In addition, the EXAFS data showed a significant level of TcS_2 present in the solid phase after 312-h oxidation (data not shown), which implies that the transformation in speciation provided only a secondary barrier that partially inhibited Tc oxidation. Once the transformation began, TcO_2 became readily available for further oxidation.

Implications. Under the batch experimental conditions of this study, oxygenation of materials containing reduced Tc resulted in considerably lower release of $Tc^{VII}O_4^-$ when the Tc had been sequestered under sulfidic conditions. However, the practical benefit of creating sulfidic conditions to sequester Tc as TcS_2 will depend on whether recalcitrance of TcS_2 to oxidation can be maintained over the long-term under field-scale remediation conditions. It should be recognized that the batch experiments used in this study represented a worst case scenario in which Tc oxidation is favored by (i) unlimited

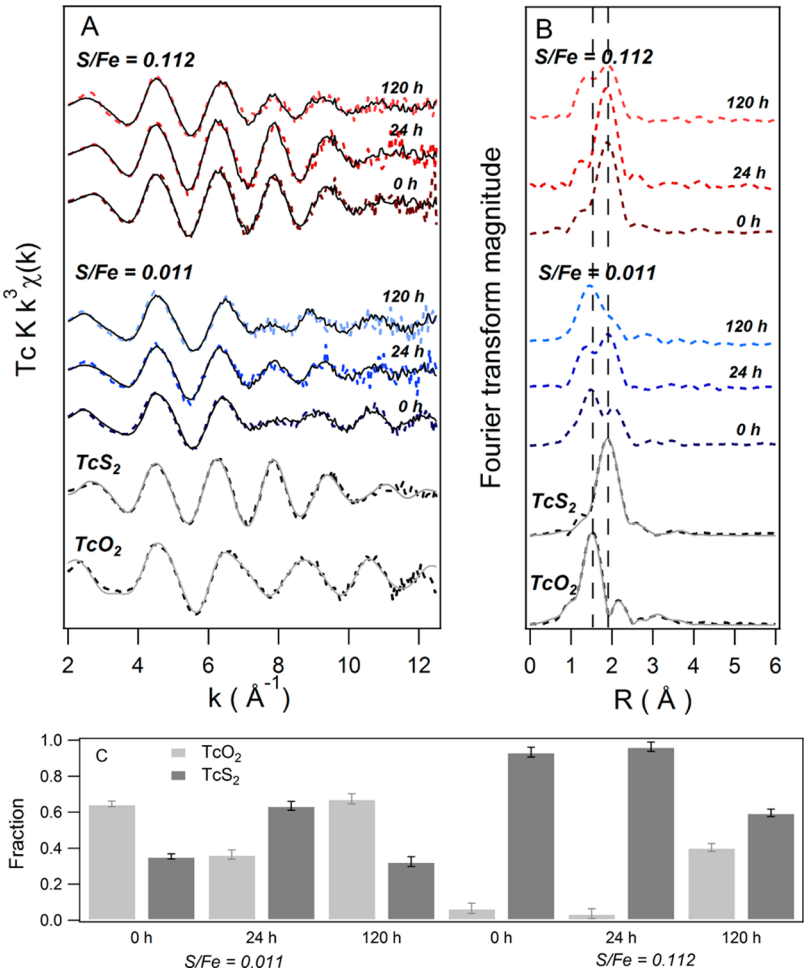

Figure 4. Tc K-edge (A) EXAFS and (B) the Fourier transformed EXAFS after 0, 24, and 120 h oxidation at S/Fe ratio = 0.011 and 0.112. Experimental data are shown by dashed lines and EXAFS fits are shown by solid lines. Vertical dashed lines in 4B denote the positions of first shell Tc—O and Tc—S binding. (C) Fraction of Tc speciation during oxidation at S/Fe = 0.011 and 0.112 based on linear combination fitting of EXAFS data (Tc reduced at S/Fe = 0 (TcO_2) and Tc reduced at S/Fe = 1.12 (TcS_2) and their respective shell-by-shell fitting were used as reference spectra.[26] Data for 0-h oxidized sample are adopted from the Tc reduction study.[26] Linear combination fitting of EXAFS of oxidized Tc at S/Fe = 0.011 and 0.112 was done using TcS_2 and TcO_2 as principle components.).

oxygen supply, (ii) no mass transport limitations, and (iii) limited redox buffer capacity of FeS. These conditions usually do not apply in the subsurface, which might make sequestration of Tc as TcS_2 more favorable under more realistic conditions. For example, the contact between reduced Tc and dissolved oxygen is likely to be limited by diffusion in vadose zone and low-flow groundwater system. Formation of secondary precipitates from iron oxidation and reprecipitation may further protect Tc from oxidation by increasing the thickness of the diffusion barrier. This effect might also explain the relatively stronger resistance to oxidation of aged samples observed in the present study. Dissolved oxygen concentration is likely to be limited due to upstream aerobic respiration by microorganisms, provided sufficient organic matter is present in aquifers. In fact, implementation of ZVI in combination with organic materials into the subsurface to stimulate in situ chemical and biological reduction has become a widely applied strategy in field remediation. With respect to the redox buffer capacity, given the general abundance of iron bearing minerals in the subsurface, the sulfidation process of these mineral phases could result in greater redox buffer capacity. Although the extent of protection exerted by these natural processes is not yet clearly understood, field data tends to show substantially less Tc mobilization than prediction derived from laboratory tests, even for TcO_2.[44]

It should be further noted that even though the high reactivity of iron sulfides for a variety of groups of subsurface contaminants has long been recognized,[45−50] FeS is commonly not considered to be stable in oxic environments. The current study may overestimate the stability of FeS and associated TcS_2 by not considering other biogeochemical processes that can oxidize FeS, such as microbially mediated oxidation (e.g., by Fe-oxidizing bacteria or nitrate-reducing bacteria) or abiotic oxidation by naturally occurring MnO_2.[51] Both of these processes have been shown to play significant roles in controlling the speciation and availability of trace metals in specific types of environments,[23,39,40] but their effects on Tc remobilization remain to be examined. Another important biogeochemical process that merits further investigation is pyritization, not only because pyrite is the ultimate sink for iron and sulfur in sulfidic environments,[52] but also because pyrite is generally considered to be less susceptible to oxidation than mackinawite. Furthermore, effective approaches to inhibit pyrite oxidation have been proposed by many prior studies,[53−55] which might be proven to be useful for further stabilization of reduced Tc sulfide.

dx.doi.org/10.1021/es501607s | Environ. Sci. Technol. 2014, 48, 7409−7417

■ ASSOCIATED CONTENT

Supporting Information

Details on the characterization and properties of original and sulfidated nZVI during oxidation and additional XAS data of Tc in unsulfidated nZVI during oxidation. This material is available free of charge via the Internet at http://pubs.acs.org.

■ AUTHOR INFORMATION

Corresponding Author

*Phone: 503-346-3431; fax: 503-346-3427; e-mail: tratnyek@ohsu.edu.

Present Address

[†]Department of Biology, Clark College, Vancouver, WA, 98663.

Notes

The authors declare no competing financial interest.

■ ACKNOWLEDGMENTS

This material is based on work supported by the Subsurface Biogeochemical Research Program of the U.S. Department of Energy, Award No. DE-SC0001376. This report has not been subject to review by the DOE and therefore does not necessarily reflect agency views and no official endorsements should be inferred. Mössbauer, XPS, μXRD, and TEM/EDS were performed using the Environmental Molecular Sciences Laboratory (EMSL), a national scientific user facility sponsored by the Department of Energy's Office of Biological and Environmental Research and located at Pacific Northwest National Laboratory. XAS was carried out at the Stanford Synchrotron Radiation Lightsource, a Directorate of SLAC National Accelerator Laboratory and an Office of Science User Facility operated for the U.S. Department of Energy Office of Science by Stanford University. The authors would like to thank Sung-Woo Lee for preliminary XAS data collection and discussion, Danielle Jansik and James Szecsody for general discussions.

■ REFERENCES

(1) Jones, T. E.; Khaleel, R.; Myers, D. A.; Shade, J. W.; Wood, M. I. A summary and evaluation of Hanford site tank farm subsurface contamination; Lockheed Martin Hanford: Richland, WA, HNF-2603, 1998.

(2) Beasley, T. M.; Dixon, P. R.; Mann, L. J. ^{99}Tc, ^{236}U, and ^{237}Np in the Snake River Plain aquifer at the Idaho National Engineering and Environmental Laboratory, Idaho Falls, Idaho. *Environ. Sci. Technol.* **1998**, *32*, 3875−3881.

(3) Icenhower, J. P.; Qafoku, N. P.; Zachara, J. M.; Martin, W. J. The biogeochemistry of technetium: A review of the behavior of an artificial element in the natural environment. *Am. J. Sci.* **2010**, *310*, 721−752.

(4) Rard, J. A. Current status of the thermodynamic data for technetium and its compounds and aqueous species. *J. Nucl. Radiochem. Sci.* **2005**, *6*, 197−204.

(5) Fredrickson, J. K.; Zachara, J. M.; Kennedy, D. W.; Kukkadapu, R. K.; McKinley, J. P.; Heald, S. M.; Liu, C.; Plymale, A. E. Reduction of TcO_4^- by sediment-associated biogenic Fe(II). *Geochim. Cosmochim. Acta* **2004**, *68*, 3171−3187.

(6) Lloyd, J. R.; Sole, V. A.; Van Praagh, C. V. G.; Lovley, D. R. Direct and Fe(II)-mediated reduction of technetium by Fe(III)-reducing bacteria. *Appl. Environ. Microbiol.* **2000**, *66*, 3743−3749.

(7) Plymale, A. E.; Fredrickson, J. K.; Zachara, J. M.; Dohnalkova, A. C.; Heald, S. M.; Moore, D. A.; Kennedy, D. W.; Marshall, M. J.; Wang, C.; Resch, C. T.; Nachimuthu, P. Competitive reduction of pertechnetate ($^{99}TcO_4^-$) by dissimilatory metal reducing bacteria and biogenic Fe (II). *Environ. Sci. Technol.* **2011**, *45*, 951−957.

(8) Pearce, C. I.; Liu, J.; Baer, D. R.; Qafoku, O.; Heald, S. M.; Arenholz, E.; Grosz, A. E.; McKinley, J. P.; Resch, C. T.; Bowden, M. E.; Engelhard, M. H.; Rosso, K. M. Characterization of natural titanomagnetites ($Fe_{3-x}Ti_xO_4$) for studying heterogeneous electron transfer to Tc(VII) in the Hanford subsurface. *Geochim. Cosmochim. Acta* **2014**, *128*, 114−127.

(9) Cui, D.; Eriksen, T. E. Reduction of pertechnetate in solution by heterogeneous electron transfer from Fe(II)-containing geological material. *Environ. Sci. Technol.* **1996**, *30*, 2263−2269.

(10) Zachara, J. M.; Heald, S. M.; Jeon, B.; Kukkadapu, R. K.; Liu, C.; McKinley, J. P.; Dohnalkova, A. C.; Moore, D. A. Reduction of pertechnetate [Tc(VII)] by aqueous Fe(II) and the nature of solid phase redox products. *Geochim. Cosmochim. Acta* **2007**, *71*, 2137−2157.

(11) Peretyazhko, T.; Zachara, J. M.; Heald, S. M.; Kukkadapu, R. K.; Liu, C.; Plymale, A. E.; Resch, C. T. Reduction of Tc(VII) by Fe(II) sorbed on Al (hydr)oxides. *Environ. Sci. Technol.* **2008**, *42*, 5499−5506.

(12) Peretyazhko, T.; Zachara, J. M.; Heald, S. M.; Jeon, B.-H.; Kukkadapu, R. K.; Liu, C.; Moore, D.; Resch, C. T. Heterogeneous reduction of Tc(VII) by Fe(II) at the solid−water interface. *Geochim. Cosmochim. Acta* **2009**, *72*, 1521−1539.

(13) Szecsody, J. E.; Jansik, D. P.; McKinley, J. P.; Hess, N. J. Influence of alkaline co-contaminants on technetium mobility in vadose zone sediments, *J. Environ. Radioact.* **2014**, [Online early access], http://dx.doi.org/10.1016/j.jenvrad.2014.1002.1003.

(14) Darab, J. G.; Amonette, A. B.; Burke, D. S. D.; Orr, R. D.; Ponder, S. M.; Schrick, B.; Mallouk, T. E.; Lukens, W. W.; Caulder, D. L.; Shuh, D. K. Removal of pertechnetate from simulated nuclear waste streams using supported zerovalent iron. *Chem. Mater.* **2007**, *19*, 5703−5713.

(15) Um, W.; Chang, H.; Icenhower, J. P.; Lukens, W. W.; Serne, R. J.; Qafoku, N. P.; Westsik, J. J. H.; Buck, E. C.; Smith, S. C. Immobilization of 99-technetium (VII) by Fe(II)-goethite and limited reoxidation. *Environ. Sci. Technol.* **2011**, *45*, 4904−4913.

(16) Maes, A.; Geraedts, K.; Bruggeman, C.; Vancluysen, J.; Rossberg, A.; Hennig, C. Evidence for the interaction of technetium colloids with humic substances by X-ray absorption spectroscopy. *Environ. Sci. Technol.* **2004**, *38*, 2044−2051.

(17) Eagling, J.; Worsfold, P. J.; Blake, W. H.; Keith-Roach, M. J. Mobilization of technetium from reduced sediments under seawater inundation and intrusion scenarios. *Environ. Sci. Technol.* **2012**, *46*, 11798−11803.

(18) McBeth, J. M.; Lear, G.; Lloyd, J. R. Technetium reduction and reoxidation in aquifer sediments. *Geomicrobiol. J.* **2007**, *24*, 189−197.

(19) Burke, I. T.; Boothman, C.; Lloyd, J. R.; Livens, F. R.; Charnock, J. M.; McBeth, J. M.; Mortimer, R. J. G.; Morris, K. Reoxidation behavior of technetium, iron, and sulfur in estuarine sediments. *Environ. Sci. Technol.* **2006**, *40*, 3529−3535.

(20) Chinni, S.; Anderson, C. R.; Ulrich, K.-U.; Giammar, D. E.; Tebo, B. M. Indirect UO_2 oxidation by Mn(II)-oxidizing spores of *Bacillus* sp. strain SG-1 and the effect of U and Mn concentrations. *Environ. Sci. Technol.* **2008**, *42*, 8709−8714.

(21) Liu, C.; Zachara, J. M.; Fredrickson, J. K.; Kennedy, D. W.; Dohnalkova, A. Modeling the inhibition of the bacterial reduction of U(VI) by β-MnO_2(s). *Environ. Sci. Technol.* **2002**, *36*, 1452−1459.

(22) Fredrickson, J. K.; Zachara, J. M.; Kennedy, D. W.; Liu, C.; Duff, M. C.; Hunter, D. B.; Dohnalkova, A. Influence of Mn oxides on the reduction of uranium(VI) by the metal-reducing bacterium *Shewanella putrefaciens*. *Geochim. Cosmochim. Acta* **2002**, *66*, 3247−3262.

(23) Wang, Z.; Lee, S.; Kapoor, P.; Tebo, B. M.; Giammar, D. E. Uraninite oxidation and dissolution induced by manganese oxide: A redox reacton between two insoluble minerals. *Geochim. Cosmochim. Acta* **2013**, *100*, 24−40.

(24) Bargar, J. R.; Williams, K. H.; Campbell, K. M.; Long, P. E.; Stubbs, J. E.; Suvorova, E. I.; Lezama-Pacheco, J. S.; Alessi, D. S.; Stylo, M.; Webb, S. M.; Davis, J. A.; Giammar, D. E.; Blue, L. Y.; Bernier-Latmani, R. Uranium redox transition pathways in acetate-amended sediments. *Proc. Natl. Acad. Sci. U.S.A.* **2013**, *110*, 4506−4511.

(25) Fredrickson, J. K.; Zachara, J. M.; Plymale, A. E.; Heald, S. M.; McKinley, J. P.; Kennedy, D. W.; Liu, C.; Nachimuthu, P. Oxidative dissolution of potential of biogenic and abiogenic TcO_2 in subsurface sediments. *Geochim. Cosmochim. Acta* **2009**, *73*, 2299−2313.
(26) Fan, D.; Anitori, R. P.; Tebo, B. M.; Tratnyek, P. G.; Lezama Pacheco, J. S.; Kukkadapu, R. K.; Engelhard, M. H.; Bowden, M. E.; Kovarik, L.; Arey, B. W. Reductive sequestration of pertechnetate ($^{99}TcO_4^-$) by nano zerovalent iron (nZVI) transformed by abiotic sulfide. *Environ. Sci. Technol.* **2013**, *47*, 5302−5310.
(27) Lee, J.-H.; Zachara, J. M.; Fredrickson, J. K.; Heald, S. M.; McKinley, J. P.; Plymale, A. E.; Resch, C. T.; Moore, D. A. Fe(II)- and sulfide-facilitated reduction of $^{99}Tc(VII)O_4^-$ in microbially reduced hyporheic zone sediments. *Geochim. Cosmochim. Acta* **2013**, *136*, 247−264.
(28) Liu, Y.; Terry, J.; Jurrison, S. Pertechnetate immobilization in aqueous media with hydrogen sulfide under anaerobic and aerobic environments. *Radiochim. Acta* **2007**, *95*, 717−725.
(29) Liu, Y.; Terry, J.; Jurrison, S. Pertechnetate immobilization with amorphous iron sulfide. *Radiochim. Acta* **2008**, *96*, 823−833.
(30) Lukens, W. W.; Bucher, J. J.; Shuh, D. K.; Edelstein, N. M. Evolution of technetium speciation in reducing grout. *Environ. Sci. Technol.* **2005**, *39*, 8064−8070.
(31) Livens, F. R.; Jones, M. J.; Hynes, A. J.; Charnock, J. M.; Mosselmans, J. F. W. X-ray absorption spectroscopy studies of reactions of technetium, uranium and neptunium with mackinawite. *J. Environ. Radioact.* **2004**, *74*, 211−219.
(32) Lee, J.-H.; Fredrickson, J. K.; Kukkadapu, R. K.; Boyanov, M. I.; Kemner, K. M.; Lin, X.; Kennedy, D. W.; Bjornstad, B. N.; Konopka, A. E.; Moore, D. A.; Resch, C. T.; Phillips, J. L. Microbial reductive transformation of phyllosilicate Fe(III) and U(VI) in fluvial subsurface sediments. *Environ. Sci. Technol.* **2012**, *46*, 3721−3730.
(33) Nurmi, J.; Sarathy, V.; Tratnyek, P.; Baer, D.; Amonette, J.; Karkamkar, A. Recovery of iron/iron oxide nanoparticles from solution: comparison of methods and their effects. *J. Nanopart. Res.* **2011**, *13*, 1937−1952.
(34) Bi, Y.; Hyun, S. P.; Kukkadapu, R.; Hayes, K. F. Oxidative dissolution of UO_2 in a simulated groundwater containing synthetic nanocrystalline mackinawite. *Geochim. Cosmochim. Acta* **2012**, *102*, 175−190.
(35) Shi, Z.; Nurmi, J. T.; Tratnyek, P. G. Effects of nano zero-valent iron (nZVI) on oxidation-reduction potential (ORP). *Environ. Sci. Technol.* **2011**, *45*, 1586−1592.
(36) Jeong, H. Y.; Han, Y.; Hayes, K. F. X-ray absorption and X-ray photoelectron spectroscopic study of arsenic mobilization during mackinawite (FeS) oxidation. *Environ. Sci. Technol.* **2010**, *44*, 955−961.
(37) Jeong, H. Y.; Han, Y.; Park, S. W.; Hayes, K. F. Aerobic oxidation of mackinawite (FeS) and its environmental implication for arsenic mobilization. *Geochim. Cosmochim. Acta* **2010**, *74*, 3182−3198.
(38) Holmes, J. Fate of incoporated metals during mackinawite oxidation in sea water. *Appl. Geochem.* **1999**, *14*, 277−281.
(39) Schippers, A.; Jørgensen, B. B. Oxidation of pyrite and iron sulfide by manganese dioxide in marine sediments. *Geochim. Cosmochim. Acta* **2001**, *65*, 915−922.
(40) Schippers, A.; Sand, W. Bacterial leaching of metal sulfides proceeds by two indirect mechanisms via thiosulfate or via polysulfides and sulfur. *Appl. Environ. Microbiol.* **1999**, *65*, 319−321.
(41) Burton, E. D.; Bush, R. T.; Sullivan, L. A. Acid-volatile sulfide oxidation in coastal flood plain drains: iron−sulfur cycling and effects on water quality. *Environ. Sci. Technol.* **2006**, *40*, 1217−1222.
(42) Hampton, M. A.; Plackowski, C.; Nguyen, A. V. Physical and chemical analysis of elemental sulfur formation during galena surface oxidation. *Langmuir* **2011**, *27*, 4190−4201.
(43) Lukens; Bucher, J. J.; Edelstein, N. M.; Shuh, D. K. Products of pertechnetate radiolysis in highly alkaline solution: Structure of $TcO_2 \cdot xH_2O$. *Environ. Sci. Technol.* **2002**, *36*, 1124−1129.
(44) Hu, Q. H.; Rose, T. P.; Zavarin, M.; Smith, D. K.; Moran, J. E.; Zhao, P. H. Assessing field-scale migration of radionuclides at the Nevada Test Site: "mobile" species. *J. Environ. Radioact.* **2008**, *99*, 1617−1630.
(45) Scheinost, A. C.; Charlet, L. Selenite reduction by mackinawite, magnetite, and siderite: XAS characterization of nanosized redox products. *Environ. Sci. Technol.* **2008**, *42*, 1984−1989.
(46) Jeong, H. Y.; Sun, K.; Hayes, K. F. Microscopic and spectroscopic characterization of Hg(II) immobilization by mackinawite (FeS). *Environ. Sci. Technol.* **2010**, *44*, 7476−7483.
(47) Veeramani, H.; Scheinost, A. C.; Monsegue, N.; Qafoku, N. P.; Kukkadapu, R.; Newville, M.; Lanzirotti, A.; Pruden, A.; Murayama, M.; Hochella, M. F. Abiotic reductive immobilization of U(VI) by biogenic mackinawite. *Environ. Sci. Technol.* **2013**, *47*, 2361−2369.
(48) Bulter, E. C.; Hayes, K. F. Factors influencing rates and products in the transformation of trichloroethylene by iron sulfide and iron metal. *Environ. Sci. Technol.* **2001**, *35*, 3884−3891.
(49) Hyun, S. P.; Davis, J. A.; Sun, K.; Hayes, K. F. Uranium(VI) reduction by iron(II) monosulfide mackinawite. *Environ. Sci. Technol.* **2012**, *46*, 3369−3376.
(50) Turcio-Ortega, D.; Fan, D.; Tratnyek, P. G.; Kim, E.-J.; Chang, Y.-S. Reactivity of Fe/FeS nanoparticles: Electrolyte composition effects on corrosion electrochemistry. *Environ. Sci. Technol.* **2012**, *46*, 12484−12492.
(51) Aller, R. C.; Rude, P. D. Complete oxidation of solid phase sulfides by manganese and bacteria in anoxic marine sediments. *Geochim. Cosmochim. Acta* **1988**, *52*, 751−765.
(52) Morse, J. W.; Millero, F. J.; Cornwell, J. C.; Rickard, D. The chemistry of the hydrogen sulfide and iron sulfide systems in natural waters. *Earth-Sci. Rev.* **1987**, *24*, 1−42.
(53) Elsetinow, A. R.; Schoonen, M. A. A.; Strongin, D. R. Aqueous geochemical and surface science investigation of the effect of phosphate on pyrite oxidation. *Environ. Sci. Technol.* **2001**, *35*, 2252−2257.
(54) Zhang, Y. L.; Evangelou, V. P. Formation of ferric hydroxide-silica coatings on pyrite and its oxidation behavior. *Soil Sci.* **1998**, *163*, 53−62.
(55) Kargbo, D. M.; Atallah, G.; Chatterjee, S. Inhibition of pyrite oxidation by a phospholipid in the presence of silicate. *Environ. Sci. Technol.* **2004**, *38*, 3432−3441.